Study of the interaction of the palmatine alkaloid with hybrid G-quadruplex/duplex and i-motif/duplex DNA structures

Noelia Ruiz[1], Petra Jarosova[2], Petr Taborsky[2*], Raimundo Gargallo[1*]

1. Department of Chemical Engineering and Analytical Chemistry, University of Barcelona, Martí I Franqués 1-11, E-08028 Barcelona, Spain
2. Department of Chemistry, Faculty of Science, Masaryk University, Kamenice 5, 62500 Brno, Czech Republic

Abstract

There is an increasing interest in the study of guanine or cytosine-rich sequences that may fold into G-quadruplex (G4) or i-motif (iM) structures showing a short hairpin (or stem-loop) stabilized by Watson-Crick base pairs. These hybrid spatial arrangements may be target of ligands that have been shown to interact strongly with B-DNA. In this work, the interaction of the palmatine alkaloid with several sequences forming different G4s, iMs, and hybrid structures has been studied by means of spectroscopic and separation techniques, as well as multivariate data analysis methods. At the experimental conditions used in this work, the results have shown that this ligand strongly stabilizes parallel G4 structures, whereas a weaker interaction was observed with the antiparallel G4 adopted by the thrombin-binding aptamer or iMs. The presence of hairpins within the loops scarcely affects the affinity of this ligand for the hybrid G4/duplex or iM/duplex structures. Fluorescence measurements have provided evidence of a certain interaction with iMs at pH 5.1, despite the absence of thermal stabilization effects.

Keywords: G-quadruplex, i-motif, hybrid structures, palmatine, binding

* Corresponding authors

PT: taborak@email.cz

RG: raimon_gargallo@ub.edu

Introduction

The most common (or canonical) DNA structure is the right-handed double helical B-DNA. Genomic research has revealed that around 98% of biological DNA is comprised of non-coding regions with important biological functions. These regions are repetitive DNA sequences that have the potential to fold into non-B DNA structures such as hairpin, G-quadruplex, i-motif, Z-DNA , H- DNA, among others under certain experimental conditions [1].

G-quadruplex (G4) structures are formed by guanine-rich sequences from DNA or RNA. G4s are based on the π-stacking of quartets of coplanar guanine bases, the so-called G-tetrads. G4 structures can adopt different topologies according to the *syn* or *anti* conformations adopted by the bases and the sugars. Accordingly, G4 can be grouped into parallel, antiparallel or mixed (3+1) topologies. The stability of G4 structures is not only strongly dependent on the hydrogen bonds existing within the G tetrads, but also on other factors, such as the nature and concentration of cations, temperature or the presence of bonded ligands [2]. Much effort is being done to understand the biological role of G4 structures [3,4], as well to develop ligands that could modulate their functions *in vivo* [5–7]. On the other hand, the i-motif (iM) is a non-B-DNA secondary structure formed by cytosine-rich DNA sequences. The core of this structure consists of two intercalated, parallel duplex strands stabilized thanks to the formation of cytosine-protonated cytosine ($C{\cdot}C^+$) pairs. As protonation of some cytosine bases is needed to form $C{\cdot}C^+$ base pairs, pH is a key factor to maintain this structure. The pK_a of cytosine is around 4.5 [8]. Therefore, iM structures are stabilized in weakly acid environment so that C bases are partially protonated.

The common characteristics of ligands interacting with G4s are the existence of a π-delocalized system that favours their stacking on the face of a G-quartet, and a partial positive charge and/or positively charged substituents to interact with the grooves and loops of G4 and the negatively charged backbone phosphates [9]. Accordingly, there are different modes of interaction: stacking on external G- quartets, groove binding, non-specific, and even intercalation in some cases [10,11]. The interaction of ligands with G4s has been studied more in deep than with iMs because biological pH (around 7) and temperature (37 ^oC) hinder the formation of stable iMs. However, recent studies have revealed the formation of iMs *in vivo* [12,13], pushing the interest in the study of these structures. The compact structure of the iM core makes very difficult the intercalation of ligands. So, the potential interactions of ligands with iMs should be non-specific with the negatively charged phosphate groups, or stacking interactions with the bases located within the loops [14,15].

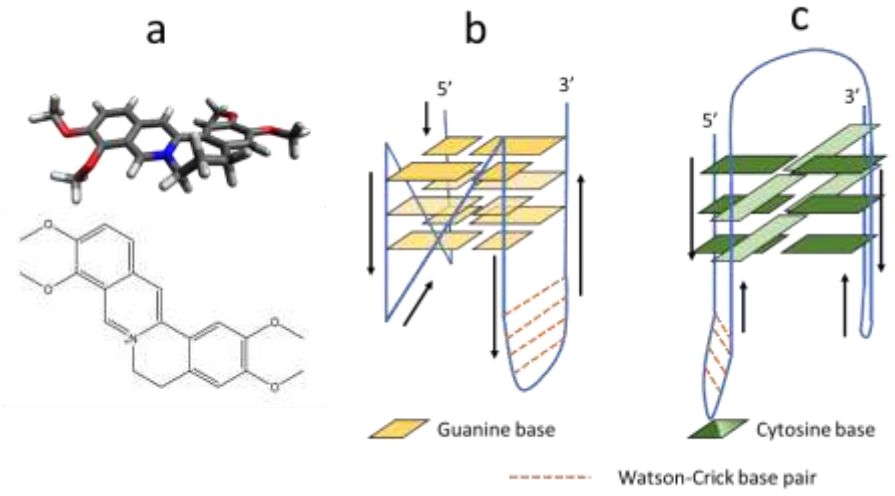

Figure 1. Three-dimensional rendering and chemical structure of palmatine (a), and proposed models for the hybrid G4/duplex structure adopted by nmyc02 (b) and for the iM/duplex structure adopted by nmyc01 (c), both of them within the *n-myc* gene [16].

The present work is a part of a project devoted to the study of the interaction of isoquinoline alkaloids with DNAs. Specially, the interaction of different DNA structures with one of these ligands, the palmatine chloride, is studied here (Figure 1). Palmatine belongs to group of protoberberine alkaloids. It is a quaternary ammonia compound as well as berberine but the structure is more opened due to the methoxy groups on positions 2 and 3 instead of methylendioxy group (present in berberine). Berberine and palmatine show also similar spectral properties having very similar emission and excitation spectra [17]. Palmatine chloride (palmatine) is isolated from plants like *Coptis chinensis* and *Phellodendron amurense*. It is the major component of herbal preparations used in traditional medicine Chinese, Korean and Indian for its properties such as anti-malarial, anti-oxidant, anti-inflammatory and low toxicity on human cells [18][19][20]. In anti-cancer therapy, as well as berberine [21], its analogue palmatine seems to inhibit the telomerase activity effectively [9][22].

In aqueous solutions palmatine shows a positive charge, which would favour the interaction with negatively charged phosphates within DNA structure. In addition, palmatine is a buckled molecule (Figure 1) that could dock on G-quartets within G4 structures, or intercalate between Watson-Crick base pairs. Hence, as berberine [23–25], it has been reported that palmatine can stabilize G4 or duplexes through binding or external stacking because of van der Waals and electrostatic attractions [26]. Bhadra and Kumar studied the interaction of palmatine with the mixed parallel/antiparallel G4 structure adopted by the human telomeric $AG_3(T_2AG_3)_3$ sequence by means of spectroscopic and calorimetric methods [27]. In 50 mM pH 6.8 buffer, 25 ^oC, and 0.1 M KCl, the interaction was shown to be 1:1 DNA:ligand with an affinity constant around 10^5 M^{-1}. In these conditions, palmatine increased in 5 ^oC the melting temperature (T_m) of the G4. Later on, the interaction with the telomeric antiparallel G4 was shown to increase the fluorescence of several alkaloids, including palmatine [28]. More recently, Comez *et al.* studied the interaction of berberine and palmatine with the $AG_3(T_2AG_3)_3$ sequence in 50 mM MES buffer, pH 7 and 100 mM KCl. By using spectroscopic techniques as well as multivariate data analysis methods, it was shown that palmatine promoted parallel conformations in detriment of antiparallel ones [29].

The interaction of palmatine with parallel G4s has also been studied. Hence, electrospray ionization mass spectrometry (ESI-MS) was used to study the interaction of palmatine with the intermolecular parallel G4 formed by $[d(TG_4T)]_4$ [30]. From the results obtained, an intercalation mechanism was proposed. A similar result was obtained when studying the interaction with G4 RNA [31]. Later on, MS was used to study the interaction with a G4 formed within the promoter region of *bcl-2* oncogene [32], being proposed a 1:3 DNA:ligand stoichiometry. The interaction of palmatine with $[d(T_2G_4T)]_4$ and $[d(T_2AG_3T)]_4$ has also been investigated using Nuclear Magnetic Resonance (NMR) [18]. The study revealed dual recognition sites in both G4 DNA sequences, resulting in thermal stabilization by 13–17 °C. Restrained molecular dynamics simulations using NOE distance restraints for 2:1 palmatine-$[d(T_2G_4T)]_4$ complex revealed end-stacking, as well as groove binding. Combining ESI-MS with CD spectroscopy, a G-rich sequence from miR-92a promoter region was discovered to form a parallel G4 structures, including a dimeric G4 structure [33]. Palmatine was shown to promote the stability of the dimeric G4 structure.

The selective interactions of synthetic derivatives of palmatine, with G4 structures has also been reported [34]. Palmatine derivatives were developed by inserting small peptide basic chains. The studies of the interactions of these compounds with various G4-forming sequences showed that the presence of suitable side chains is very useful for improving the interaction of the ligands with G4 structures.

To our knowledge, the interaction of palmatine with G4 or iM structures showing a short hairpin fragment within a loop has not been studied yet. This could be of interest because of the unique structural characteristics of the boundary between the G4 or iM core and the Watson-Crick stabilized hairpin, which could be a convenient site for ligand binding [35–38]. Previously, the formation of these hybrid structures was proposed for two sequences (nmyc01 and nmyc02) found near the promoter region of the *n-myc* gene [16] (Table 1). In the present work, the interaction of palmatine with these sequences has been studied by

means of different instrumental techniques, as well as multivariate data analysis methods. Also, it has been investigated the interaction of the ligand with two mutated sequences (nmyc01m and nmyc02m), where some bases within a loop have been mutated to thymine to prevent the formation of the Watson-Crick stabilized hairpin. For comparison, the interaction with parallel and antiparallel G4s, as well as iM and duplex structures has also been studied. The results have shown that this ligand stabilizes parallel G4 structures, whereas a weaker interaction was observed with the antiparallel G4 adopted by the thrombin binding aptamer. No interaction of palmatine with iMs was observed. Finally, the interaction of palmatine with a parallel G4 structure showing the presence of an internal hairpin is similar to that observed for a similar G4 lacking such hairpin.

Materials and methods

Reagents

Palmatine was obtained from plant material in the Department of Biochemistry, Masaryk University (Brno, Czech Rep.) The DNA sequences (Table 1) were synthesized on an Applied Biosystems 3400 DNA synthesizer using the 1 µM scale synthesis cycle. Standard phosphoramidites were used. Ammonia deprotection was performed overnight at 55°C. The resulting products were purified using Glen-Pak Purification Cartridge (Glen Research, Sterling, VA, USA). The integrity of DNA sequences was checked by means of Mass Spectrometry. DNA strand concentration was determined by absorbance measurements (260 nm) at 90 ^{o}C using the extinction coefficients calculated using the nearest-neighbour method as implemented on the OligoCalc webpage [39]. Before any experiment, DNA solutions were first heated to 95^{o}C for 20 minutes and then allowed to reach room temperature overnight. 100 mM phosphate buffer (pH 7.1, Sigma-Aldrich, Merck KGaA, Darmstadt, Germany), and 3 M acetate buffer (pH 5.1, Sigma-Aldrich, Merck KGaA, Darmstadt, Germany) stock solutions were used to prepare the samples for measurements (10 mM buffer, 5 mM KCl).

DNA name	Sequence (5'→3')	Expected structure	References
nmyc02	AGG GGG TGG GAG GGG GCA TGC AGA TGC AGG GGG T	Parallel G4 / duplex	[16]
nmyc02m	AGG GGG TGG GAG GGG GCT TTT TGA TGC AGG GGG T	Parallel G4	[16]
ckit21T12T21	CGG GCG GGC GCT AGG GAG GGT	Parallel G4	[40]
Pu22T14T23	TGA GGG TGG GAG GGT GGG GAA A	Parallel G4	[40]
TBA	GGT TGG TGT GGT TGG	Antiparallel G4	[41]
C3TA2	CCC TAA CCC TAA CCC TAA CCC T	iM at pH 5	[42]
nmyc01	ACC CCC TGC ATC TGC ATG CCC CCT CCC ACC CCC T	iM / duplex at pH 5	[16]
nmyc01m	ACC CCC TGC ATC TTT TTG CCC CCT CCC ACC CCC T	iM at pH 5	[16]
T20	TTT TTT TTT TTT TTT TTT TT	Unfolded	

Table 1. DNA sequences studied in this work. The column labelled "Expected structure" refers to the structure adopted by the considered sequence at low temperature, 10 mM phosphate buffer (pH 7.1), and 5 mM KCl, apart from cytosine-rich sequences (C3TA2, nmyc01 and nmyc01m) where 10 mM acetate buffer (pH 5.1) was considered.

Instruments

Absorbance spectra were recorded on an Agilent 8453 spectrophotomer. For absorbance measurements, a quartz cuvette with an optical path length of 1 cm, and 1400 μL volume (Hellma, Jena, Germany) was used. The temperature of the cuvette was controlled with an Agilent 89090A Peltier device. CD spectra were recorded on a Jasco J-810 spectropolarimeter. In this case, a quartz cuvette with an optical path length of 1 cm, and 3000 μL volume was used. The temperature was controlled with a JULABO F-25- HD device. Fluorescence spectra were recorded on an Aminco-Bowman series 2 spectrofluorimeter equipped with a xenon lamp. The excitation wavelength was set to 360 nm and the emission wavelength was to 530 nm with a sensibility of 700 or 800V. A quartz cuvette with an optical path length of 1 x 0.4 cm, and 1000 μL volume was used. The temperature was controlled with a JULABO F-25- HD device.

SE-HPLC measurements were done on Waters 2695 HPLC equipped with a degasser, a quarternary pump, an autosampler, a photodiode array detector and a SEC-S-3000 as a SE-HPLC column. A pH 7.1 buffer (5 mM KCl and 10 mM potassium phosphate) mobile phase was used. To characterize DNA structures, 15 μL of samples at 20 ^{o}C were injected with a flow rate of 0.8 mL/min. DNA and palmatine concentrations were 2 and 6 μM, respectively, and were prepared in 10 mM potassium phosphate (pH 7.1) and 5 mM KCl.

Methods

CD-monitored melting experiments were measured from 5-15 to 90-95 ^{o}C, depending on the studied system. In addition to the ellipticity measured at a single wavelength (265, 280 or 292 nm, depending on the DNA structure), a set of CD spectra were recorded every 5^{o}C. A temperature ramp of 0.6 ^{o}C·min^{-1} was used. DNA and palmatine concentrations were 2 and 6 μM, respectively. The spectrum of the blank was removed from the recorded spectra.

Spectroscopically-monitored titrations of DNA with palmatine were performed by adding increasing volumes of a 60 μM palmatine stock solution to a 600 μL solution of the corresponding DNA (2 μM). All these solutions were prepared in 10 mM buffer and 5 mM KCl. The temperature was controlled with a water bath at 20 ^{o}C.

Data analysis

CD-monitored melting experiments provided two data sets: a table of *m* CD spectra recorded at *n* wavelengths (data matrix **D**), and a table of *p* ellipticity values at a selected wavelength measured at *p* temperatures.

Data matrix **D** was analyzed with a multivariate method, as described elsewhere [16,43]. Briefly, this method allows the determination of the number of components (*nc*) present along the melting, and the calculation of the distribution diagram (**C**), and spectra (**S**) of the *nc* components present in that experiment. This calculation was made by using an implementation of the Lambert-Beer law for multivariate data:

$$\boldsymbol{D}\ (m\ x\ n) = \boldsymbol{C}(m\ x\ nc) * \boldsymbol{S}(nc\ x\ n) + \boldsymbol{E}(m\ x\ n) \quad \text{(Equation 1)}$$

In this equation, the dimensions of each matrix are given between parentheses. The matrix **E** contains residual data not explained by the proposed model of *nc* components. Prior to this analysis, CD spectra in matrix **D** were smoothed using a Savitzky-Golay filter, as implemented in Matlab computing software (The Mathworks Inc., Natick, MA, USA). The components in Equation 1 may be related to the different conformations present along the melting. In all cases studied in this work, *nc* was equal to 2, i.e., no intermediates (at least, spectroscopically-active in CD) were resolved with this procedure. The table of ellipticity values measured at a single wavelength was also analyzed to determine the melting temperature (T_m) of the transition

[44]. In this case, the baseline drifts were removed prior to the analysis and a two-state process was assumed. The T_m value was determined from the least-squares fitting of a sigmoidal curve to the processed data by using the cftool Toolbox in Matlab.

For the analysis of binding equilibria, fluorescence spectra recorded along the titrations of DNA with palmatine were analyzed by means of the Equispec program [45], another method for multivariate analysis. As in the previous case, this program decomposes the matrix containing the experimentally-measured spectra into three matrices, which contain the distribution diagram, the spectra and the residual fluorescence data not explained by the proposed model of species (Equation 1). Goodness of fit was evaluated by calculating the r^2 and the lack-of-fit (%) according to:

$$lack\ of\ fit = 100\sqrt{\frac{\sum(F_i - F_{i,calc})^2}{\sum F_i^2}} \qquad \text{(Equation 2)}$$

In this equation, F_i and $F_{i,calc}$ are the experimental and fitted fluorescence values, respectively.

Results and discussion

Scarce structural modifications upon interaction with palmatine

Firstly, the interaction of palmatine with the selected sequences was studied qualitatively by means of CD spectroscopy and SE-HPLC. CD spectra of some G4 forming sequences (Pu22T14T23, TBA, nmyc02 and myc02) are shown in Figure 2. The CD spectra of Pu22T14T23, nmyc02 and nmyc02m showed positive and negative signals at 262 and 245 nm, approximately. These signatures have been assigned to parallel G4 conformations [46]. The CD spectrum of ckit21T12T21 also shows the characteristics of a parallel G4 (Figure S1a). Otherwise, the CD spectrum of TBA showed positive signals at 292 and 245 nm, and a negative signal at 267 nm (Figure 2b), which were related to an antiparallel G4 conformation [46]. In presence of palmatine (1:3 DNA:ligand ratio), little changes were observed in the UV region of the CD spectra. This fact suggests that the overall structure of the G4 was maintained upon interaction with the ligand. Only Pu22T14T23 and nmyc02 showed small changes. On the other hand, no induced signals were observed in the visible region of the CD spectra in any case, which points to a weak interaction that does not produce changes in the chirality of the ligand.

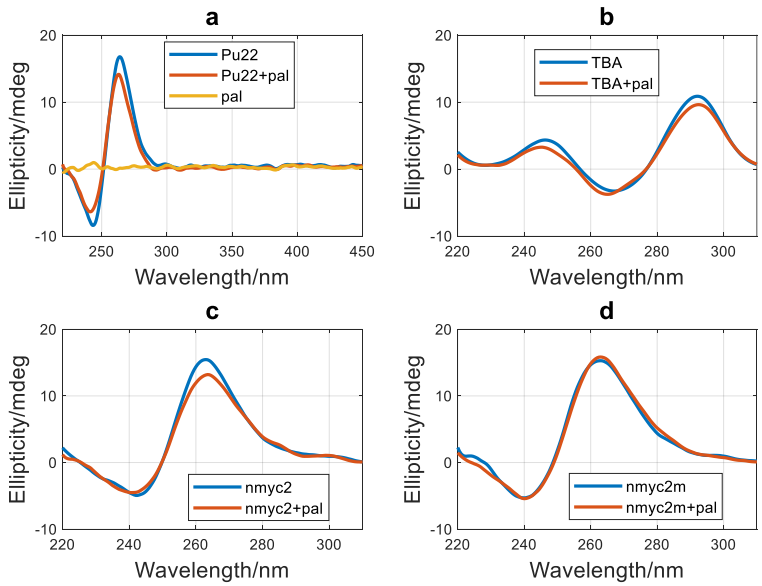

Figure 2. CD spectra of G4 and G4:ligand mixtures. (a) Pu22T14T23, (b) TBA, (c) nmyc02, (d) nmy02m. DNA concentration was 2 μM, ligand concentration was 6 μM, 5 mM KCl, 10 mM phosphate buffer, pH 7.1, 20 °C.

Whereas long cytosine-rich sequences, such as those studied in this work, fold into monomer iM structures, G4-forming sequences may adopt monomer structures but also, dimer, tetramer or even higher-order aggregates, such as G-wires [47]. CD spectroscopy provides an overall picture of the structure adopted by a sequence but it does not provide information about the molecularity of the structures formed. SE-HPLC chromatography is a separation technique that provides a clue on molecularity of the structures adopted by DNA sequences at experimental conditions very similar to those of spectroscopic measurements [48]. Figure 3 shows the chromatograms obtained for some of the G4-forming sequences. The chromatograms of ckit21T12T21, nmyc02 and nmyc02m showed the presence of two bands, which reflects the formation of structures of different molecularity. On the other hand, both Pu22T14T23 and TBA showed the presence of only one band. The number of strands involved in each band was deduced from the calibration plot of the $\log_{10}$(MW) against V_e/V_0 [48], where V_e and V_0 are the elution and dead volumes, respectively. According to this graph, the elution bands observed for the ckit21T12T21 sample corresponded to monomer (10.3 minutes) and dimer (9.6 minutes) structures. The bands observed in the chromatograms of Pu22T14T23 and TBA at 10.6 minutes were assigned to the monomer G4. Finally, the bands observed in the case of nmyc02 and nmyc02m samples were assigned to the monomer (10.2 minutes) and to a broad envelope of aggregates [16]. In all cases, the chromatograms recorded for the DNA:palmatine (1:3) mixtures only revealed very small changes in the polymorphism of the considered G4-forming sequences.

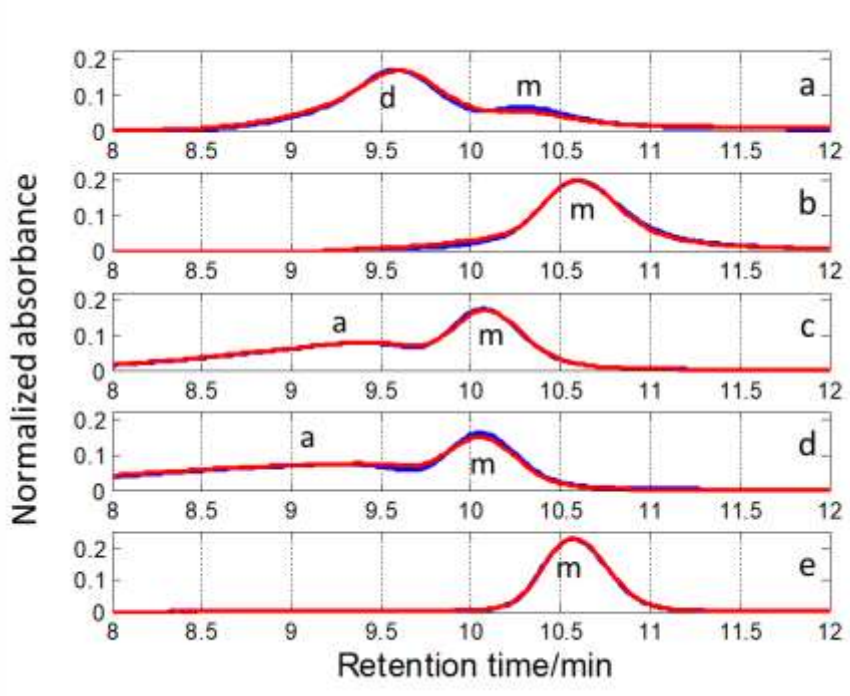

Figure 3. Normalized SE-HPLC chromatograms of DNAs (blue) and 1:3 DNA:ligand mixures (red) . (a) ckit21T12T21, (b) Pu22T14T23, (c) nmyc02, (d) nmy02m, (e) TBA. “m”, “d” and “a” stands for “monomer”, “dimer” and “aggregates”. Experimental conditions were 2 μM DNA, 6 μM ligand, 10 mM phosphate buffer and 5 mM KCl, 20 ^{o}C.

To gain insight into the stabilizing potential of palmatine, a series of CD-monitored melting experiments were carried out. From these, it may be deduced whether the ligand binds more tightly to the folded or unfolded forms of each sequence. As described in the experimental section, not only the variation of ellipticity at selected wavelengths was monitored, but also a set of CD spectra were measured along the melting experiment (Figures S2 and S3). The values of the melting temperatures (T_m) associated to the unfolding process were determined from the transformed ellipticity curves by considering a two-state approach (Figure S4). This assumption was checked by applying multivariate analysis to the sets of CD spectra.

As example, the melting experiment of the 1:3 nmyc01:palmatine mixture at pH 5.1 is explained here. Some of the measured spectra along this experiment are shown in Figure 4a, whereas the complete set is included in Figure S3. This last data set was analyzed by means of a multivariate data analysis method to determine the number of spectroscopically-active components present along the melting experiment [43], as well as their corresponding distribution diagram and spectra. These components were assigned to the different DNA conformations present along the melting, as palmatine does not show any CD signal. In the case of the 1:3 nmyc01:palmatine mixture, two significant components were observed, which were assigned to the folded and unfolded conformations of DNA. Considering this number of components, the corresponding distribution diagram (Figure 4b) and CD spectra (Figure 4c) were calculated. Finally, Figure 4d shows the calculated and experimental ellipticity values at 285 nm, reflecting that the proposed model of two components fits well the experimental data. The analysis was also carried out for a large number of components but the obtained results were not meaningful. Once the assumption of a two-state process was confirmed, the ellipticity *vs*. temperature curve was transformed into the fraction of folded DNA *vs*. temperature (Figure S4). From this curve, the T_m value was determined (Table 2).

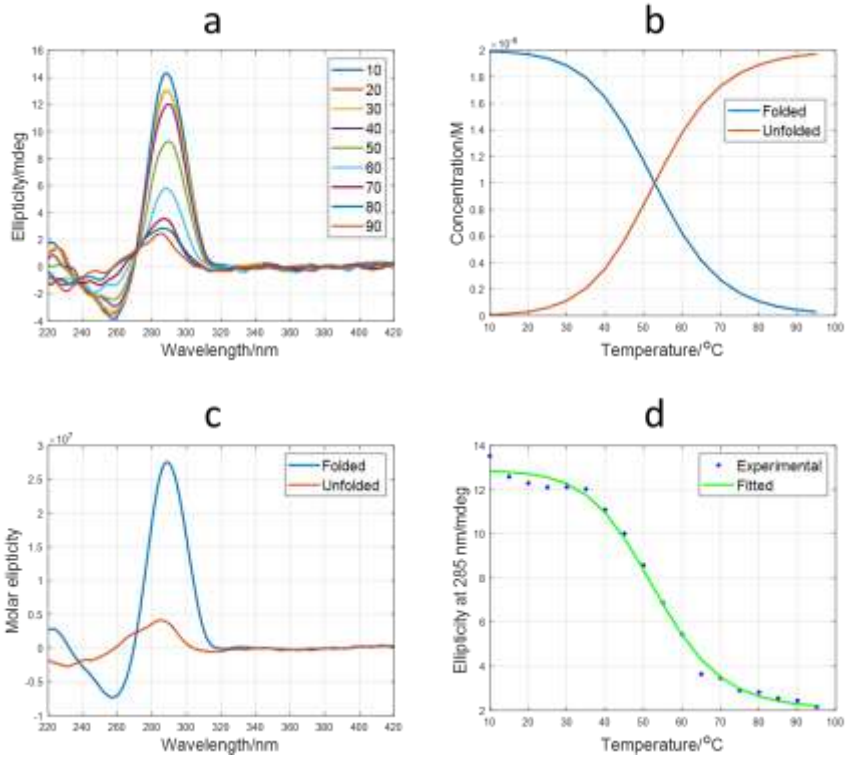

Figure 4. Melting experiment of the nmyc01:palmatine (1:3) mixture at pH 5.1. (a) Selected CD spectra. Inset: temperature values. DNA and palmatine concentration were 2 and 6 μM, respectively; (b) Calculated distribution diagram for the two components proposed; (c) Calculated spectra for the two components proposed. (d) Fitted versus experimental ellipticity values at 285 nm.

The experimental conditions used in the melting experiments consisted in 10 mM phosphate buffer (pH 7), and 5 mM KCl. This relatively low concentration of potassium ion was chosen to prevent the extraordinary stabilization of G4 structures, especially parallel G4, which would hinder the study of the stabilizing potential of palmatine. Concerning parallel G4s, the most stable structure is that adopted by Pu22T14T23 (76.5 ^{o}C). Other sequences (ckit21T12T21, nmyc02 or nmyc02m) also form stable structures with T_m values around 55 ^{o}C. In presence of palmatine, T_m values increase dramatically (ΔT_m > 14.5 ^{o}C), which reflects a clear stabilization of the parallel G4 structures, as already pointed by other authors [34]. In addition, the ΔT_m value was similar (within the experimental error) for the mixture of the ligand with nmyc02 (a hybrid parallel G4 with Watson-Crick hairpin) and

for the mixture with nmyc02m (a parallel G4 that does not show such hairpin). Therefore, it was deduced that the presence of the internal hairpin within the G4 adopted by nmyc02 does not yield an additional stabilization of the resulting G4:palmatine complex, in relation to that observed for the G4 structure lacking that hairpin (nmyc02m). Finally, only a small increase was observed in the case of the antiparallel G4 structure adopted by TBA (4.2 ^{o}C). This smaller stabilization could be due to a certain selectivity of the ligand for parallel G4s, or from the fact that TBA has only two G-tetrads instead of three in all other G-quadruplex structures.

	Expected structure	T_m (^{o}C)	T_m (^{o}C)	ΔT_m (^{o}C)
pH 7.1				
ckit21T12T21	Dimeric parallel G4	59.0 ± 0.8	76.9 ± 1.0	17.9 ± 1.8
Pu22T14T23	Parallel G4	76.5 ± 0.7	~ 94	> 17.5
TBA	Antiparallel G4	44.3 ± 0.5	48.8 ± 0.5	4.2 ± 1.0
nmyc02	Parallel G4 with Watson-Crick hairpin	56.8 ± 0.5	73.1 ± 0.8	16.3 ± 1.3
nmyc02m	Parallel G4	57.1 ± 0.6	72.7 ± 0.7	15.6 ± 1.3
nmyc01	Hairpin	32.4 ± 0.8	33.1 ± 1.1	0.7 ±1.9
nmyc01m	Hairpin	21.6 ± 0.7	21.5 ± 0.7	-0.1 ± 1.4
nmyc01 : nmyc02	Watson-Crick duplex	66.8± 0.4	~ 85	> 18.2
nmyc01m : nmyc02m	Watson-Crick duplex with internal bulge	54.9 ± 0.4	81 ± 2	26.1 ± 2.4
pH 5.1				
C_3TA_2	iM	56.4 ± 0.8	56.2 ± 0.7	-0.2 ± 1.5
nmyc01	iM with Watson-Crick hairpin	54.2 ± 0.7	52.7 ± 1.0	0.5 ± 1.7
nmyc01m	iM	54.0 ± 0.6	53.9 ± 0.6	-0.1 ± 1.2

Table 2. Determined T_m values from the melting experiments of DNA and DNA:ligand mixtures. DNA concentration was 2 μM, 10 mM phosphate (pH 7.1) or acetate (pH 5.1) buffer, 5 mM KCl. Palmatine concentration was 6 μM in all cases, except for duplex and duplex with internal bulge (9 μM).

At pH 7.1, the meltings of the cytosine-rich sequences nmyc01 and nmyc01m were characterized by smaller values of T_m values than those determined for G4 structures. This fact was related to the formation of partially folded structures, such as hairpins. By using Nupack software [49], the structure and stability of these structures were calculated (Figure S5). It is expected that, at the experimental conditions used in this work (10 mM phosphate buffer, 5 mM KCl, 20 ^{o}C) both, partially folded and unfolded strands coexist. On the other hand, the formation of very stable iM structures by nmyc01 or nmyc01m at this pH is probably not possible due to several reasons, like the length of cytosine stretches in these sequences, and the nature and length of the loops [50][51]. In this sense, it is clear that nmyc01 forms a relatively more stable structure than nmy01m. Upon addition of palmatine, and considering the associated uncertainties in ΔT_m values, the structure adopted by nmyc01 was not more stabilized than that formed by nmyc01m.

For comparison, the interaction of palmatine with the B-DNA formed by the 1:1 mixture of nmyc01 and nmyc02 at pH 7.1 was studied. As expected, the value of ΔT_m could not be determined accurately because of the large stabilization provided by the ligand. Also, the melting of the 1:1 mixture of the mutated sequences nmyc01m and nmyc02m was carried out. In this case, as both sequences show a five-long stretch of thymine bases, the duplex contains an internal bulge, probably stabilized by T·T base pairs. The presence of such internal bulge produces a clear reduction of the stability in relation to the non-mutated mixture (54.9 vs. 66.8 ^{o}C). The addition of the ligand also produced a clear stabilization of the mutated duplex (ΔT_m = 26.1 ^{o}C).

The effect of palmatine on the structures adopted by nmyc01 and nmyc01m at pH 5.1 were also studied. At this pH, the iM was observed to be the major structure [16]. The determined T_m values were high (around 54 ^oC), which confirms the key role of pH on the stabilization of iMs. The C_3TA_2 sequence forms an iM of similar stability, which points out to the formation of a similar number of $C{\cdot}C^+$ base pairs (six) in all three cases. Upon addition of palmatine, ΔT_m was near 0 for C_3TA_2 and nmyc01m, and 0.5 for nmyc01. Considering the uncertainty associated to T_m determination, it was deduced that palmatine has no effect on the stability of iM structures, even in the case of the hybrid iM/duplex structure.

Binding constants

Palmatine has a weak fluorescence emission at 530 nm, which may be dramatically enhanced upon interaction with DNA [52]. Therefore, the interaction of palmatine with G4, iM and hybrid structures was also studied by means of molecular fluorescence-monitored titrations in order to determine the stoichiometry and association constants of the formed complexes (Figures S6 and S7). Figure 5 shows the relative fluorescence intensity measured for samples consisting on DNA and palmatine (1:3 ratio). At pH 7, it was observed that the fluorescence of palmatine was higher in the presence of G-quadruplex and duplex structures than in the presence of cytosine-rich sequences. At pH 5.1 (where iMs are the major structures), fluorescence intensity is slightly higher than at pH 7.1.

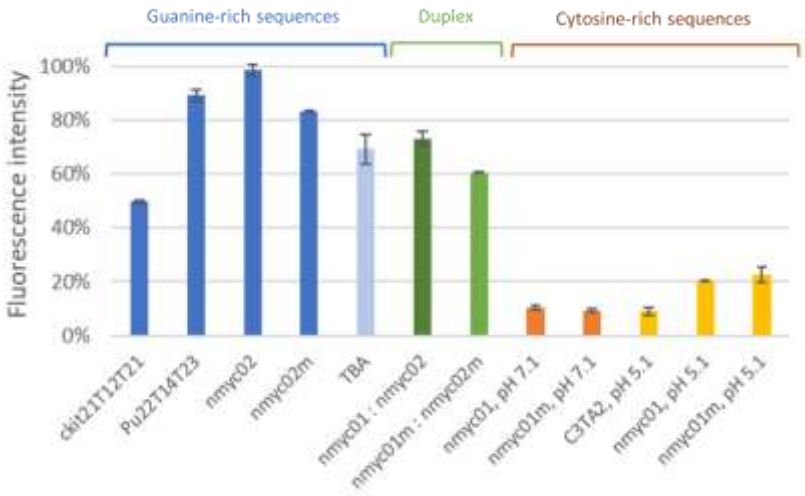

Figure 5. Fluorescence relative intensity of DNA:palmatine mixtures. The DNA and palmatine concentrations were 2 and 6 μM, respectively. Samples were prepared in 10 mM phosphate or acetate buffer, 5 mM KCl, and 20 ^oC. All fluorescence intensities were measured at the same voltage (700 V).

Figure 6a shows the spectra measured along the titration of nmyc01 at pH 5.1 with palmatine. An increase of fluorescence was observed along the titration. The set of spectra were analyzed by means of the Equispec program in order to determine the number of different complexes formed along the experiment, as well as their distribution diagrams and spectra [45]. This analysis showed that the experimental data could be satisfactorily explained considering a non-cooperative 1:1 (DNA:ligand) binding (logarithm of the binding constant equal to 5.14±0.06). The calculated distribution diagram and spectra are shown in Figure 6b and 6c, respectively. Figure 6d shows the fitted versus experimental fluorescence intensities at 530 nm. The 1:1 stoichiometry was also checked by means of the Job's plot (Figure S8).

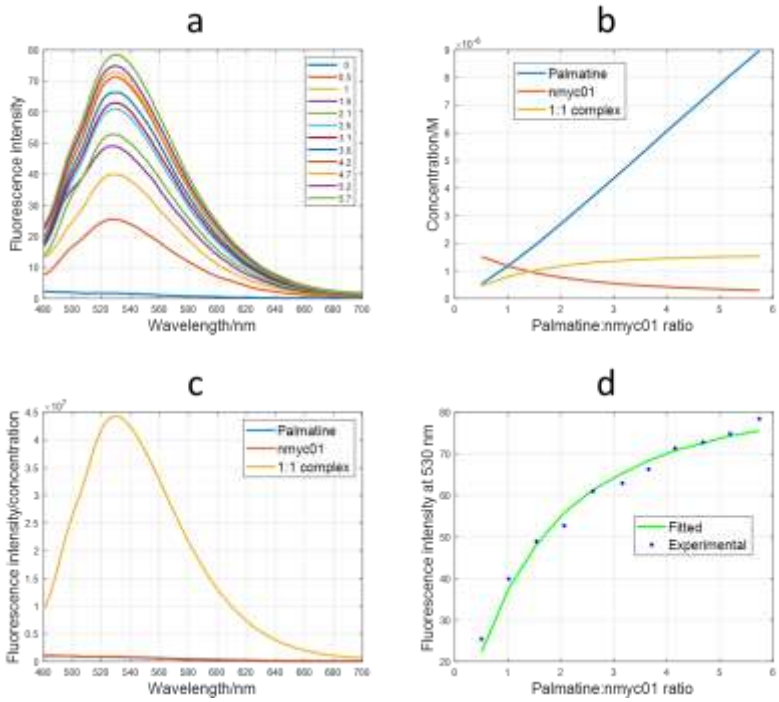

Figure 6. Titration of nmyc01 with palmatine at pH 5.1. (a) Fluorescence spectra. Inset: palmatine:nmyc01 ratio. DNA concentration was 2 μM, 20 °C, 800 V; (b) Calculated distribution diagram for the three species proposed; (c) Calculated spectra for the three species proposed. (d) Fitted versus experimental fluorescence intensity values at 530 nm.

Table 3 summarizes the values of the determined binding constants, as well as the lack of fit, which is a measure of the quality of the fitting procedure. For all the considered sequences and mixtures, the spectroscopic data were well fitted to a non-cooperative 1:1 binding, whereas other stoichiometries provided higher values of the lack of fit parameter. This 1:1 stoichiometry agrees with previous reports on the interaction of palmatine with the $AG_3(T_2AG_3)_3$ telomeric sequence [27], and with guanine-rich sequences forming tetramolecular G4 structures [18].

pH 7.1	**Logarithm of the binding constant**	**lack of fit (%)**
ckit21T12T21	6.24±0.07	3.0
Pu22T14T23	6.80±0.18	3.5
TBA	5.73±0.02	1.6
nmyc02	6.30±0.05	3.2
nmyc02m	6.32±0.05	3.5
nmyc01	5.14±0.06	2.0
nmyc01m	4.74±0.03	1.3
nmyc01:nmyc02	6.04±0.04	3.3
nmyc01m:nmyc02m	6.00±0.04	3.4
pH 5.2	**Logarithm of the binding constant**	**lack of fit (%)**
C3TA2	5.34±0.06	3.5
nmyc01	5.76±0.05	3.9
nmyc01m	5.41±0.02	1.4
nmyc01:nmyc02	5.88±0.04	2.9

Table 3. Values of the association constant K_A, as well as their corresponding uncertainties (95 % confidence level) and fitting parameters, calculated for the interaction between berberine and the selected DNA sequences.

At pH 7.1 and at 20 ^{o}C, stronger interactions were observed for duplex and for G4 structures. The weaker interactions were observed for nmyc01 and nmyc01m, which are mainly present as a partially folded hairpin, as shown previously. For G4 structures, the binding constants are around $10^{6.3}$ – $10^{6.8}$ M^{-1}, which denote a relatively strong binding. In a previous work, Franceschin *et al.* reported an affinity constant equal to $10^{5.49}$ M^{-1} for the interaction of palmatine with a parallel G4 structure found near the promoter of the *c-kit* gene in 10 mM tris-HCl buffer and 100 mM of KCl [34]. This smaller value of the binding constant determined by these authors could be related to the greater content of salt used in their experiments, which would produce a reduction of the electrostatic interactions between charged ligand and DNA [17]. No differences were observed between the binding affinity of palmatine for nmyc02 (parallel G4 with Watson-Crick hairpin) or nmyc02m (parallel G4 without any hairpin), which could be explained as a result of a similar affinity of the ligand for the G4 and hybrid moieties within the structure adopted by nmyc02. Finally, the affinity constant determined for the interaction of palmatine with the antiparallel G4 structure adopted by TBA was slightly smaller than those determined for ckit21T12T21, nmyc02 or nmyc02m. This result is in agreement with the smaller ΔT_m value determined in the case of the TBA:palmatine mixture than in the case of the mixtures with parallel G4 structures. Overall, these results pointed out to a greater interaction with parallel than with the antiparallel G4 structure adopted by TBA.

The interaction of palmatine with the perfect duplex (nmyc01:nmyc02) and with the mismatched duplex (nmyc01m:nmyc02m) was very similar, and slightly weaker than with the G4 structures. At pH 5.2, the binding with the perfect duplex was also weaker than at pH 7.1, probably due to the disruption of the duplex to yield the intramolecular G4 and iM structures.

At pH 7.1, the interaction of palmatine with cytosine-rich sequences is very weak, being the binding constant for the palmatine:nmyc01 interaction slightly higher than for the mutated sequence. This could be related to the slightly greater stability of the hairpin formed by nmyc01 in relation to nmyc01m. At pH 5.2, the interaction of the ligand with the iMs is characterized by an increase of the fluorescence (Figure 7) and for a higher value of the binding constant. This increase of the fluorescence intensity in presence of an iM structure could be used to develop analytical methodology to detect it, as shown already by using other ligands [53]. The determined binding constant, however, was lower than those determined for G4s or duplex structures, and similar to that previously reported for the berberine alkaloid [17]. Again, the binding constant for the interaction of palmatine with the iM/duplex hybrid structure is slightly higher than with the structure lacking the internal hairpin.

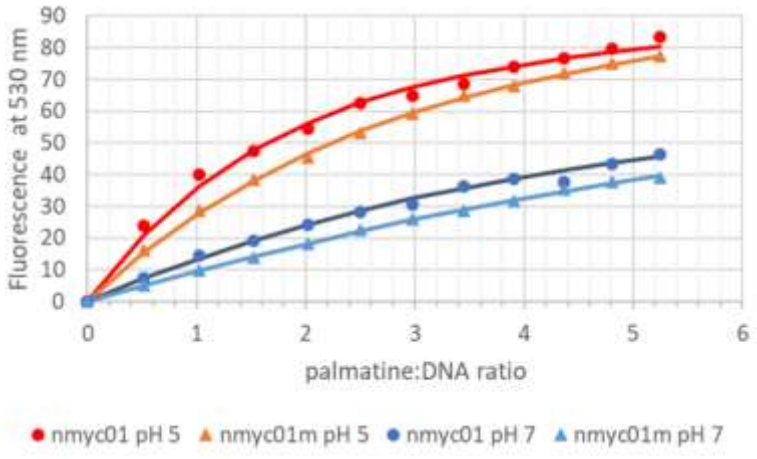

Figure 7. Binding curves for nmyc01 and nmyc01m at pH 5.1 and 7.1 (20^{o}C, 800 V). Symbols are the experimental values, whereas lines represent the fitted values considering a 1:1 DNA:palmatine interaction model.

Conclusions

In this work, the interaction of palmatine ligand with a series of G4, iM and duplex structures has been studied by means of spectroscopic and separation techniques. The results have shown that this ligand interacts more strongly with parallel than with the antiparallel G4 structure adopted by the thrombin binding aptamer. However, no changes were observed within the DNA structures upon interaction with the ligand, which points out to a mode of binding based on stacking on external G-tetrads. In the case of the G4/duplex hybrid structure, such as that formed by the nmyc02 sequence, the presence of an internal hairpin within the G4 structure has no effect on the interaction with the ligand. Palmatine has also been shown to stabilize strongly duplex structures, including those showing internal bulges.

In the case of iM structures, the addition of the ligand produced a clear increase of the fluorescence emission at pH 5.2 in relation to that observed at pH 7.1, where the iM unfolds. However, the binding is very weak, as deduced from melting and binding experiments, which pointed out to a mode of interaction rather based on electrostatic interaction, rather than on intercalation. As in the case of the G4/duplex hybrid formed by nmyc02, the presence of a hairpin within the iM structure has no effect on stabilization due to ligand binding.

Acknowledgements

This investigation was supported by research grant from the Spanish *Ministerio de Ciencia e Innovación* (PID2019-107158GB-I00). Nuria Pfennig (UB) is thanked for carrying out some of the experiments. Dra. Anna Aviñó and Dr. Ramon Eritja (IQAC-CSIC, Barcelona) are thanked for providing some of the DNAs studied in this work.

Bibliography

[1] S. Neidle, S. Balasubramanian, eds., Quadruplex Nucleic Acids, RSC Publishing, Cambridgeç, 2006. http://linkinghub.elsevier.com/retrieve/pii/0302459880870267.

[2] J. Spiegel, S. Adhikari, S. Balasubramanian, The Structure and Function of DNA G-Quadruplexes, Trends Chem. (2019). https://doi.org/10.1016/J.TRECHM.2019.07.002.

[3] N. Kosiol, S. Juranek, P. Brossart, A. Heine, K. Paeschke, G-quadruplexes: a promising target for cancer therapy, Mol. Cancer. 20 (2021). https://doi.org/10.1186/s12943-021-01328-4.

[4] M. Tassinari, S.N. Richter, P. Gandellini, Biological relevance and therapeutic potential of G-quadruplex structures in the human noncoding transcriptome, Nucleic Acids Res. 49 (2021) 3617–3633. https://doi.org/10.1093/nar/gkab127.

[5] T. Santos, G.F. Salgado, E.J. Cabrita, C. Cruz, G-quadruplexes and their ligands: Biophysical methods to unravel g-quadruplex/ligand interactions, Pharmaceuticals. 14 (2021). https://doi.org/10.3390/ph14080769.

[6] I. Alessandrini, M. Recagni, N. Zaffaroni, M. Folini, On the road to fight cancer: The potential of g-quadruplex ligands as novel therapeutic agents, Int. J. Mol. Sci. 22 (2021). https://doi.org/10.3390/ijms22115947.

[7] T. Vy Thi Le, S. Han, J. Chae, H.-J. Park, G-Quadruplex Binding Ligands: from Naturally Occurring to Rationally Designed Molecules, Curr. Pharm. Des. 18 (2012) 1948–1972. https://doi.org/10.2174/138161212799958431.

[8] S. Benabou, A. Aviñó, R. Eritja, C. González, R. Gargallo, Fundamental aspects of the nucleic acid i-motif structures, RSC Adv. 4 (2014) 26956–26980. https://doi.org/10.1039/C4RA02129K.

[9] X. Ji, H. Sun, H. Zhou, J. Xiang, Y. Tang, C. Zhao, The Interaction of Telomeric DNA and C-myc22 G-Quadruplex with 11 Natural Alkaloids, Nucleic Acid Ther. 22 (2012) 127–136. https://doi.org/10.1089/nat.2012.0342.

[10] M. Kaushik, A. Singh, M. Kumar, S. Chaudhary, S. Ahmed, S. Kukreti, Structure-Specific Ligand Recognition of Multistranded DNA Structures, Curr. Top. Med. Chem. 17 (2016) 138–147. https://doi.org/10.2174/1568026616666160530154239.

[11] C. Wei, G. Jia, J. Yuan, Z. Feng, C. Li, A Spectroscopic Study on the Interactions of Porphyrin with G-Quadruplex DNAs, Biochemistry. 45 (2006) 6681–6691. https://doi.org/10.1021/bi052356z.

[12] S. Dzatko, M. Krafcikova, R. Hänsel-Hertsch, T. Fessl, R. Fiala, T. Loja, D. Krafcik, J.-L.L. Mergny, S. Foldynova-Trantirkova, L. Trantirek, Evaluation of stability of DNA i-motifs in the nuclei of living mammalian cells, Angew. Chemie - Int. Ed. 57 (2018) 2165–2169. https://doi.org/10.1002/anie.201712284.

[13] M. Zeraati, D.B. Langley, P. Schofield, A.L. Moye, R. Rouet, W.E. Hughes, T.M. Bryan, M.E. Dinger, D. Christ, I-motif DNA structures are formed in the nuclei of human cells, Nat. Chem. 10 (2018) 631–637. https://doi.org/10.1038/s41557-018-0046-3.

[14] H. Abou Assi, M. Garavís, C. González, M.J. Damha, i-Motif DNA: structural features and significance to cell biology, Nucleic Acids Res. 46 (2018) 8038–8056. https://doi.org/10.1093/nar/gky735.

[15] S.S. Masoud, K. Nagasawa, i-Motif-Binding Ligands and Their Effects on the Structure and Biological Functions of i-Motif, Chem. Pharm. Bull. 66 (2018) 1091–1103. https://doi.org/10.1248/cpb.c18-00720.

[16] S. Benabou, R. Ferreira, A. Aviñó, C. González, S. Lyonnais, M. Solà, R. Eritja, J. Jaumot, R. Gargallo, Solution equilibria of cytosine- and guanine-rich sequences near the promoter region of the n-myc gene that contain stable hairpins within lateral loops, Biochim. Biophys. Acta - Gen. Subj. 1840 (2014) 41–52. https://doi.org/10.1016/j.bbagen.2013.08.028.

[17] R. Gargallo, A. Aviñó, R. Eritja, P. Jarosova, S. Mazzini, L. Scaglioni, P. Taborsky, Study of alkaloid berberine and its interaction with the human telomeric i-motif DNA structure, Spectrochim. Acta - Part A Mol. Biomol. Spectrosc. 248 (2021) 119185. https://doi.org/10.1016/j.saa.2020.119185.

[18] P. Kumar, R. Barthwal, Structural and biophysical insight into dual site binding of the protoberberine alkaloid palmatine to parallel G-quadruplex DNA using NMR, fluorescence and Circular Dichroism spectroscopy, Biochimie. 147 (2018) 153–169. https://doi.org/10.1016/j.biochi.2018.02.002.

[19] D. Tarabasz, W. Kukula-Koch, Palmatine: A review of pharmacological properties and pharmacokinetics, Phyther. Res. 34 (2020) 33–50. https://doi.org/https://doi.org/10.1002/ptr.6504.

[20] J. Long, J. Song, L. Zhong, Y. Liao, L. Liu, X. Li, Palmatine: A review of its pharmacology, toxicity and pharmacokinetics, Biochimie. 162 (2019) 176–184. https://doi.org/https://doi.org/10.1016/j.biochi.2019.04.008.

[21] M.A. Samad, M.Z. Saiman, N. Abdul Majid, S.A. Karsani, J.S. Yaacob, Berberine Inhibits Telomerase Activity and Induces Cell Cycle Arrest and Telomere Erosion in Colorectal Cancer Cell Line, HCT 116, Mol. . 26 (2021). https://doi.org/10.3390/molecules26020376.

[22] Y.-J. Ho, J.-W. Lu, Y.-L. Huang, Z.-Z. Lai, Palmatine inhibits Zika virus infection by disrupting virus binding, entry, and stability, Biochem. Biophys. Res. Commun. 518 (2019) 732–738. https://doi.org/https://doi.org/10.1016/j.bbrc.2019.08.120.

[23] A. Pagano, N. Iaccarino, M.A.S. Abdelhamid, D. Brancaccio, E.U. Garzarella, A. Di Porzio, E. Novellino, Z.A.E. Waller, B. Pagano, J. Amato, A. Randazzo, Common G-quadruplex binding agents found to interact with i-motif-forming DNA: Unexpected multi-target-directed compounds, Front. Chem. 6 (2018) 1–13. https://doi.org/10.3389/fchem.2018.00281.

[24] M. Franceschin, L. Rossetti, A. D'Ambrosio, S. Schirripa, A. Bianco, G. Ortaggi, M. Savino, C. Schultes, S. Neidle, Natural and synthetic G-quadruplex interactive berberine derivatives, Bioorganic Med. Chem. Lett. 16 (2006) 1707–1711. https://doi.org/10.1016/j.bmcl.2005.12.001.

[25] A. Arora, C. Balasubramanian, N. Kumar, S. Agrawal, R.P. Ojha, S. Maiti, Binding of berberine to human telomeric quadruplex - Spectroscopic, calorimetric and molecular modeling studies, FEBS J. 275 (2008) 3971–3983. https://doi.org/10.1111/j.1742-4658.2008.06541.x.

[26] Y.X. Xiong, Z.S. Huang, J.H. Tan, Targeting G-quadruplex nucleic acids with heterocyclic alkaloids and their

derivatives, Eur. J. Med. Chem. 97 (2015) 538–551. https://doi.org/10.1016/j.ejmech.2014.11.021.

[27] K. Bhadra, G.S. Kumar, Interaction of berberine, palmatine, coralyne, and sanguinarine to quadruplex DNA: A comparative spectroscopic and calorimetric study, Biochim. Biophys. Acta - Gen. Subj. 1810 (2011) 485–496. https://doi.org/10.1016/j.bbagen.2011.01.011.

[28] L. Zhang, H. Liu, Y. Shao, C. Lin, H. Jia, G. Chen, D. Yang, Y. Wang, Selective Lighting Up of Epiberberine Alkaloid Fluorescence by Fluorophore-Switching Aptamer and Stoichiometric Targeting of Human Telomeric DNA G-Quadruplex Multimer, Anal. Chem. 87 (2015) 730–737. https://doi.org/10.1021/ac503730j.

[29] L. Comez, F. Bianchi, V. Libera, M. Longo, C. Petrillo, F. Sacchetti, F. Sebastiani, F. D'Amico, B. Rossi, A. Gessini, C. Masciovecchio, H. Amenitsch, C. Sissi, A. Paciaroni, Polymorphism of human telomeric quadruplexes with drugs: a multi-technique biophysical study, Phys. Chem. Chem. Phys. 22 (2020) 11583–11592. https://doi.org/10.1039/D0CP01483D.

[30] N. Xu, H. Yang, M. Cui, F. Song, Z. Liu, S. Liu, Evaluation of alkaloids binding to the parallel quadruplex structure [d(TGGGGT)]4 by electrospray ionization mass spectrometry, J. Mass Spectrom. 47 (2012) 694–700. https://doi.org/10.1002/jms.2997.

[31] W. Tan, G. Yuan, Electrospray ionization mass spectrometric exploration of the high-affinity binding of three natural alkaloids with the mRNA G-quadruplex in the BCL2 5'-untranslated region, Rapid Commun. Mass Spectrom. 27 (2013) 560–564. https://doi.org/10.1002/rcm.6484.

[32] C. Qian, H. Fu, K.A. Kovalchik, H. Li, D.D.Y. Chen, Specific Binding Constant and Stoichiometry Determination in Free Solution by Mass Spectrometry and Capillary Electrophoresis Frontal Analysis, Anal. Chem. 89 (2017) 9483–9490. https://doi.org/10.1021/acs.analchem.7b02443.

[33] M. Xi, Y. Li, J. Zhou, Exploration of the formation and structure characteristics of a miR-92a promoter G-quadruplex by ESI-MS and CD, Talanta. 211 (2020) 120708. https://doi.org/10.1016/j.talanta.2019.120708.

[34] M. Franceschin, L. Cianni, M. Pitorri, E. Micheli, S. Cacchione, C. Frezza, M. Serafini, M.-H. Hu, H. Su, Z. Huang, L. Gu, A. Bianco, Natural Aromatic Compounds as Scaffolds to Develop Selective G-Quadruplex Ligands: From Previously Reported Berberine Derivatives to New Palmatine Analogues, Molecules. 23 (2018) 1423. https://doi.org/10.3390/molecules23061423.

[35] T.Q. Ngoc Nguyen, K.W. Lim, A.T. Phan, Duplex formation in a G-quadruplex bulge, Nucleic Acids Res. 48 (2020) 10567–10575. https://doi.org/10.1093/nar/gkaa738.

[36] I. Serrano-Chacón, B. Mir, N. Escaja, C. González, Structure of i-Motif/Duplex Junctions at Neutral pH, J. Am. Chem. Soc. 143 (2021) 12919–12923. https://doi.org/10.1021/jacs.1c04679.

[37] E. Ruggiero, S. Lago, P. Šket, M. Nadai, I. Frasson, J. Plavec, S.N. Richter, A dynamic i-motif with a duplex stem-loop in the long terminal repeat promoter of the HIV-1 proviral genome modulates viral transcription, Nucleic Acids Res. 47 (2019) 11057–11068. https://doi.org/10.1093/nar/gkz937.

[38] L. Shi, P. Peng, J. Zheng, Q. Wang, Z. Tian, H. Wang, T. Li, I-Motif/miniduplex hybrid structures bind

benzothiazole dyes with unprecedented efficiencies: A generic light-up system for label-free DNA nanoassemblies and bioimaging, Nucleic Acids Res. 48 (2020) 1681–1690. https://doi.org/10.1093/nar/gkaa020.

[39] W.A. Kibbe, Oligo Calc: an online oligonucleotides properties calculator, Nucleic Acids Res. 35 (2007) W43–W46. https://doi.org/10.1093/nar/gkm234.

[40] P. Jarosova, P. Paroulek, M. Rajecky, V. Rajecka, E. Taborska, R. Eritja, A. Aviñó, S. Mazzini, R. Gargallo, P. Taborsky, Naturally occurring quaternary benzo[: C] phenanthridine alkaloids selectively stabilize G-quadruplexes, Phys. Chem. Chem. Phys. 20 (2018) 21772–21782. https://doi.org/10.1039/c8cp02681e.

[41] S. Nagatoishi, Y. Tanaka, K. Tsumoto, Circular dichroism spectra demonstrate formation of the thrombin-binding DNA aptamer G-quadruplex under stabilizing-cation-deficient conditions, Biochem. Biophys. Res. Commun. 352 (2007) 812–817. https://doi.org/10.1016/j.bbrc.2006.11.088.

[42] S. Fernández, R. Eritja, A. Aviñó, J. Jaumot, R. Gargallo, Influence of pH, temperature and the cationic porphyrin TMPyP4 on the stability of the i-motif formed by the 5'-(C3TA2)4-3' sequence of the human telomere, Int. J. Biol. Macromol. 49 (2011) 729–736. https://doi.org/10.1016/j.ijbiomac.2011.07.004.

[43] R. Gargallo, Hard/Soft hybrid modeling of temperature-induced unfolding processes involving G-quadruplex and i-motif nucleic acid structures, Anal. Biochem. 466 (2014) 4–15. https://doi.org/10.1016/j.ab.2014.08.008.

[44] J.D. Puglisi, I.B.T.-M. in E. Tinoco, [22] Absorbance melting curves of RNA, in: RNA Process. Part A Gen. Methods, Academic Press, 1989: pp. 304–325. https://doi.org/https://doi.org/10.1016/0076-6879(89)80108-9.

[45] R.M. Dyson, S. Kaderli, G. a Lawrance, M. Maeder, a D. Zunderbuhler, Second order global analysis: the evaluation of series of spectrophotometric titrations for improved determination of equilibrium constants, Anal. Chim. Acta. 353 (1997) 381–393. https://doi.org/Doi 10.1016/S0003-2670(97)87800-2.

[46] J. Kypr, I. Kejnovská, D. Renčiuk, M. Vorlíčková, Circular dichroism and conformational polymorphism of DNA, Nucleic Acids Res. 37 (2009) 1713–1725. https://doi.org/10.1093/nar/gkp026.

[47] J.L. Huppert, Structure, location and interactions of G-quadruplexes, FEBS J. 277 (2010) 3452–3458. https://doi.org/10.1111/j.1742-4658.2010.07758.x.

[48] E. Largy, J.L. Mergny, Shape matters: Size-exclusion HPLC for the study of nucleic acid structural polymorphism, Nucleic Acids Res. 42 (2014) e149–e149. https://doi.org/10.1093/nar/gku751.

[49] J.N. Zadeh, C.D. Steenberg, J.S. Bois, B.R. Wolfe, M.B. Pierce, A.R. Khan, R.M. Dirks, N.A. Pierce, NUPACK: Analysis and design of nucleic acid systems, J. Comput. Chem. 32 (2011) 170–173. https://doi.org/https://doi.org/10.1002/jcc.21596.

[50] M. McKim, A. Buxton, C. Johnson, A. Metz, R.D. Sheardy, Loop Sequence Context Influences the Formation and Stability of the i-Motif for DNA Oligomers of Sequence (CCCXXX)4, where X = A and/or T, under Slightly

Acidic Conditions, J. Phys. Chem. B. 120 (2016) 7652–7661. https://doi.org/10.1021/acs.jpcb.6b04561.

[51] S.P. Gurung, C. Schwarz, J.P. Hall, C.J. Cardin, J.A. Brazier, The importance of loop length on the stability of i-motif structures, Chem. Commun. 51 (2015) 5630–5632. https://doi.org/10.1039/C4CC07279K.

[52] M. Maiti, G.S. Kumar, Polymorphic nucleic acid binding of bioactive isoquinoline alkaloids and their role in cancer, J. Nucleic Acids. 2010 (2010). https://doi.org/10.4061/2010/593408.

[53] H. Chen, H. Sun, W. Zhang, Q. Zhang, J. Ma, Q. Li, X. Guo, K. Xu, Y. Tang, Chelerythrine as a fluorescent light-up ligand for an i-motif DNA structure, New J. Chem. 45 (2021) 28–31. https://doi.org/10.1039/D0NJ04863A.